Biomechanical Simulation to Compare the Blood Hemodynamics and Cerebral Aneurysm Rupture Risk in Patients with Different Aneurysm Necks

Article *in* Journal of Applied Mechanics and Technical Physics · November 2017

DOI: 10.1134/S0021894417060025

CITATIONS
7

READS
43

4 authors, including:

Keyvan Hajirayat
Islamic Azad University Tehran North Branch
4 PUBLICATIONS **21** CITATIONS
SEE PROFILE

Seifollah Gholampour
Islamic Azad University Tehran North Branch
36 PUBLICATIONS **164** CITATIONS
SEE PROFILE

Davood Bizari
Trauma Research Center
17 PUBLICATIONS **205** CITATIONS
SEE PROFILE

ISSN 0021-8944, Journal of Applied Mechanics and Technical Physics, 2017, Vol. 58, No. 6, pp. 968–974. © Pleiades Publishing, Ltd., 2017.
Original Russian Text © K. Hajirayat, S. Gholampour, I. Sharifi, D. Bizari.

BIOMECHANICAL SIMULATION TO COMPARE THE BLOOD HEMODYNAMICS AND CEREBRAL ANEURYSM RUPTURE RISK IN PATIENTS WITH DIFFERENT ANEURYSM NECKS

K. Hajirayat[a,b], S. Gholampour[b], I. Sharifi[a], and D. Bizari[a]

UDC 616

Abstract: In this study, one normal subject and two patients suffering from a cerebral aneurysm with circular and elliptical necks are analyzed by using the fluid-structure interaction (FSI) method. Although the blood hemodynamics parameters increase after the occurrence of the disease, the largest increase is in the wall shear stress (by a factor of 4.1–6.5) as compared to the normal subject. The increase in these parameters for patients with a circular neck is more pronounced than that with an elliptical neck. The blood flow becomes slightly more turbulent after the occurrence of the cerebral aneurysm, though it still remains in the range of the laminar flow and the pulsatility of the blood flow in patients is 28–45% greater than that of the normal subject. Finally, the results show that the risk of vessel rupture in the cerebral aneurysm with a circular neck is 40.8% higher than that in the case of the cerebral aneurysm with an elliptical neck.

Keywords: cerebral aneurysm, aneurysm rupture, fluid-structure interaction, Reynolds number, Womersley number, wall shear stress, blood hemodynamics.

DOI: 10.1134/S0021894417060025

INTRODUCTION

A cerebral aneurysm is a blood-filled bulge in vessel walls in anterior and posterior of the Willis circle [1]. This disease is the cause of one of the most common strokes, which is induced by rupture of the cerebral aneurysm in the subarachnoid area, increasing the rate of mortality [2].

Research carried out in the field of hemodynamics of the aneurysm can be divided into two categories. The first group includes studies that use computational fluid dynamics (CFD) methods. Steinman et al. [3] evaluated the blood velocity and compared vortices created in the input of the aneurysm area between normal subjects and patients [3]. Shojima et al. [4] introduced the wall shear stress (WSS) as an index to predict the risk of aneurysm rupture. Valencia et al. [5] in their research showed that the blood flow in vessels with an aneurysm should be studied by using a non-Newtonian fluid model. They assumed that the vessel walls were rigid and imposed the no-slip condition on the boundary between the blood flow and vessel walls; moreover, the vessel walls were also assumed to displace in accordance with the heart rate. For this reason, a more realistic assumption for the boundary conditions between the blood flow and vessel walls is the fluid-structure interaction (FSI) model. Therefore, the FSI method is used in the second category of research to analyze the aneurysm instead of CFD. Hajirayat et al. [6] and Valencia et al. [7] used numerical simulation to evaluate the blood hemodynamics parameters in the cerebral vessel of a normal subject and a patient with an aneurysm. Baek et al. [8] compared the oscillatory behavior of the

[a]Biomedical Research Center, Baqiyatallah University of Medical Science, Tehran, Iran; k.hajirayat@iau-tnb.ac.ir; imansharifi@aut.ac.ir; bizari.d82@gmail.com. [b]Department of Biomedical Engineering, North Tehran Branch, Islamic Azad University, Tehran, Iran; s.gholampour@iau-tnb.ac.ir. Translated from Prikladnaya Mekhanika i Tekhnicheskaya Fizika, Vol. 58, No. 6, pp. 16–22, November–December, 2017. Original article submitted September 21, 2016.

WSS vector in patients with different cerebral aneurysm sizes by using the FSI method. Brinjikji et al. [9] showed that the aneurysm size is an important and effective factor in selecting a suitable method for treatment of these patients.

It is worth noting that the effect of aneurysm size changes on the hemodynamics parameters of blood was investigated in previous studies. In the present study, however, we investigate the influence of the geometrical shape of the aneurysm neck on the blood hemodynamics parameters by using the FSI method and evaluate the aneurysm rupture risk in patients with different aneurysm necks.

1. MATERIALS AND METHODS

In this study, two patients suffering from a cerebral aneurysm in the middle cerebral artery (curved-shaped vessel in the head) and one normal subject were recruited. Models A, B, and C correspond to the normal subject, patient suffering from a cerebral aneurysm with a circular neck, and patient suffering from a cerebral aneurysm with an elliptical neck, respectively. After preparing MRI files and extracting point clouds from the head of three subjects, three-dimensional modeling of subjects' heads was performed in the SOLIDWORKS software (2014 SP3.0). It should be noted that the diameter of the aneurysm neck in model B was 2.6 mm; the small and large diameters of the aneurysm neck in model C were 3.5 and 6 mm, respectively. The dome diameter in the patients was 6 mm, and the main artery diameters in all subjects were 4 mm.

The ABAQUS 6.13 software was used for meshing and problem solving.

The continuity and steady-state Navier–Stokes equations governing the fluid (blood) model in the Eulerian space are solved [10, 11]:

$$\nabla \cdot V = 0, \qquad \frac{\partial \rho V}{\partial t} + \nabla \cdot (\rho V V) = \nabla \cdot \sigma.$$

Here ρ, V, and σ are the density, velocity vector, and Cauchy stress tensor of the blood flow, respectively. The equations used for modeling the vessel wall material are based on Hooke's law in the Lagrangian space [12]:

$$\sigma = 2\mu\varepsilon + \lambda \operatorname{tr}(\varepsilon) I.$$

Here λ and μ are the Lamé coefficients and ε and I are strain and identity tensors, respectively.

The FSI boundary conditions on the vessel walls are

$$d_i^f = d_i^s, \qquad n \cdot \tau_{ij}^f = n \cdot \tau_{ij}^s, \qquad u = \dot{d}_1^s, \tag{1}$$

where d_i^s and τ_{ij}^s are the displacement and shear stress tensor of the vessel walls and d_i^f and τ_{ij}^f are the same parameters for the blood flow. Equations (1) are kinematic, kinetic, and velocity boundary conditions, respectively.

According to [5], the Newtonian and incompressible assumptions were used in the blood flow simulation. The blood viscosity and density were 0.004 Pa $\cdot$ s and 1050 kg/m^3, respectively. The mechanical properties of the vessel walls also include Young's modulus equal to 3 MPa, density of 2300 kg/m^3, and Poisson's ratio equal to 0.49. The amplitude of the input flow was 0.21 m/s and the frequency was 1.61 Hz [7]; the pressure of the output flow was zero [13]. A tetrahedral mesh was used for the fluid (blood) model, and a triangular mesh was applied for the solid (vessel) model. The difference between the blood velocity obtained on the fine and medium meshes of three subjects in models A, B, and C was smaller than 2.1% (Fig. 1).

2. RESULTS

For testing the algorithm, we first compared the calculated diagrams of the blood velocity in the aneurysm neck of both patients and the diagram of the blood velocity in the main artery of the normal subject with the corresponding diagrams measured by the Cine phase contrast magnetic resonance imaging (Cine PC-MRI). The error at the maximum and minimum of velocity in the diagrams is smaller than 4.2%, which testifies that the model adequately describes the phenomenon and the boundary conditions are applied correctly.

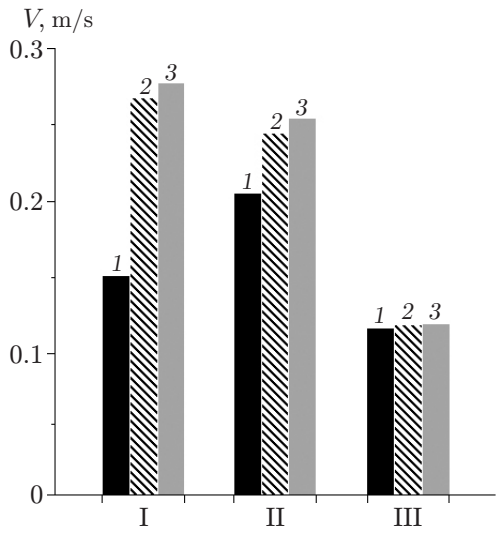

Fig. 1.

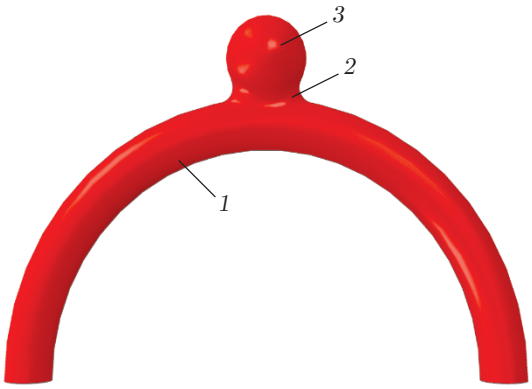

Fig. 2.

Fig. 1. Blood flow velocities calculated on different meshes: coarse mesh (*1*), medium mesh (*2*), and fine mesh (*3*); the results are given for the patient with a circular neck of the aneurysm (I), patient with an elliptical neck of the aneurysm (II), and normal subject (III).

Fig. 2. Model of the main artery with an aneurysm: (*1*) main artery; (*2*) neck; (*3*) aneurysm dome.

2.1. Investigation of the Blood Flow

Figure 2 shows the model of the main artery with an aneurysm. The blood velocity distributions in models B and C are shown in Figs. 3a and 3b, respectively. The locations of the maximum blood velocity of all subjects are in the main artery: 0.199, 0.268, and 0.245 m/s for models A, B, and C, respectively. Therefore, after the occurrence of a cerebral aneurysm, the blood velocities in the patients with circular and elliptical necks were 34.7 and 23.1% greater than that for the normal subject. It means that the blood velocity for the patient with a circular neck was higher than that for the patient with an elliptical neck with a difference of 9.4%. The maximum blood velocity calculated for the patient suffering from a cerebral aneurysm with a circular neck in [14] was 0.230 m/s. The difference from the present results is 14.2%, which can be attributed to differences both in the anatomical conditions of subjects and in the solution methods and boundary conditions of the two studies. In the present study, the vessel walls are assumed deformable according to the real conditions of arteries in the body, and the FSI method is used. Shishir et al. [14] assumed the vessel walls to be rigid, imposed the no-slip boundary condition, and used CFD for the analysis.

The place of occurrence of the maximum flow rate is in the main artery of the subjects. The maximum blood flow rate in the normal subject and patients B and C are $2.5 \cdot 10^{-6}$, $3.4 \cdot 10^{-6}$, and $3.1 \cdot 10^{-6}$ m^3/s, respectively. The Reynolds number $\mathrm{Re} = \rho^f u D/\mu$ (D is the aqueduct diameter) for the normal subject is 208.9, while this number in patients with circular and elliptical necks is greater by 34.7 and 23.1%, respectively. After occurrence of the aneurysm, the blood flow in both patients still remains in the range of the laminar flow, though the Reynolds number increases.

2.2. Investigation of the Blood Pressure

Another important hemodynamics parameter in the study of the cerebral aneurysm disease is the blood pressure. Figures 3c and 3d show the blood pressure distributions in models B and C, respectively. Similar to the maximum blood flow velocity, the maximum blood pressure occurs in the main artery; these pressures in the normal subject and patients B and C are 51.2, 75.0, and 70.0 Pa, respectively. This means that the maximum blood pressure in patients with circular and elliptical necks is higher than that of the normal subject by 46.5 and 36.7%, respectively. Hence, the type of the aneurysm neck produces a minor effect (about 6.7%) on the maximum blood pressure.

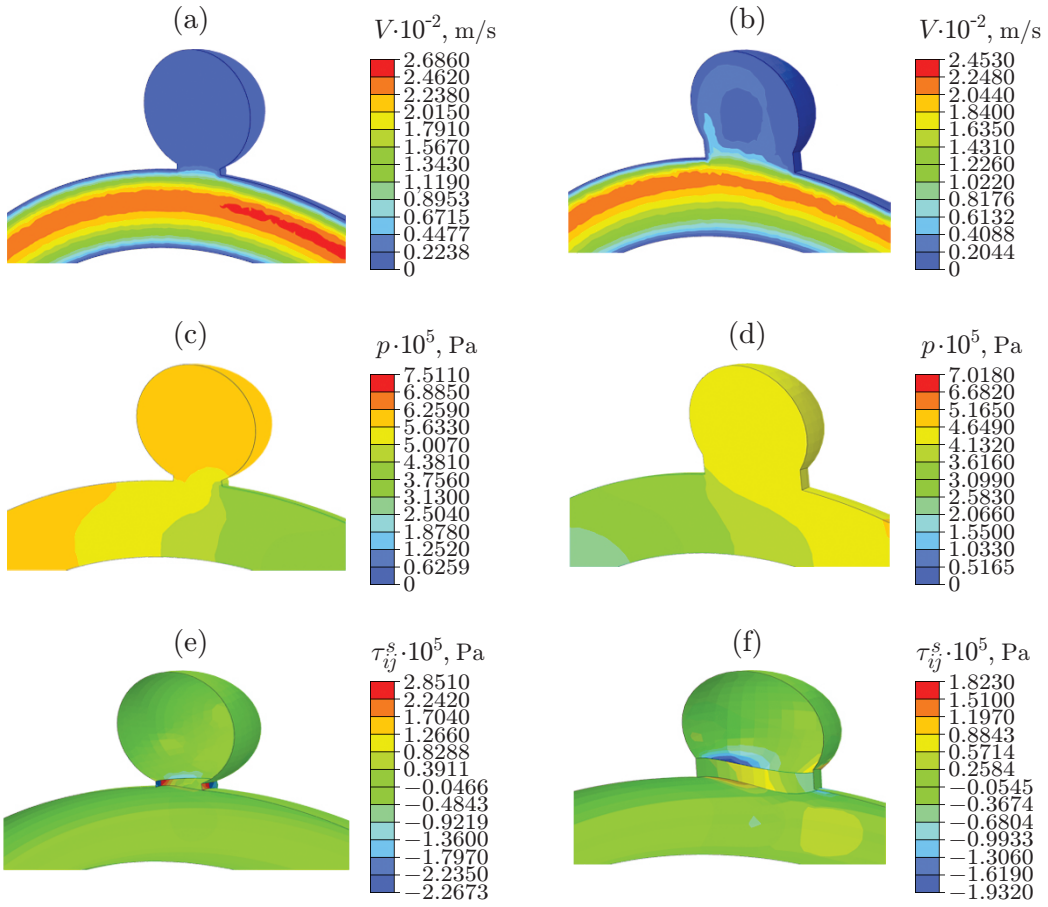

Fig. 3. Distributions of the blood flow velocity V (a and b), pressure p (c and d), and wall shear stress τ_{ij}^{s} (e and f) for patients B (a, c, and e) and C (b, d, and f).

The maximum pressures in the aneurysm neck and aneurysm dome of the patient with a circular neck are 43.6 and 41.5 Pa; these values for the patient with an elliptical neck are 34.6 and 32.5 Pa, respectively.

2.3. Investigation of the Wall Shear Stress

Figures 3e and 3f show the blood WSS distribution in models B and C, respectively. The maximum WSS values in the aneurysm neck of patients B and C are 28.5 and 18.2 Pa, respectively. The maximum WSS values for the patients with circular and elliptical necks are 6.5 and 4.1 times greater than that for the normal subject, and the maximum WSS for the patient with a circular neck is 1.6 times that for the patient with an elliptical neck. Torii et al. [15] calculated the maximum WSS in a patient suffering from a cerebral aneurysm with a circular neck by using the FSI method. The value was 30 Pa, which was 5.3% higher than the maximum WSS in the present study. The cause of this difference is the difference in the anatomical conditions of the examined subjects in the two studies. The WSS in other areas of the patients' brain is also higher than that of the normal subject. For example, the maximum WSS in the main artery of the normal subject and patients B and C are 4.4, 6.4, and 4.5 Pa, respectively. This means that the maximum WSS values in the main artery of the patients with circular and elliptical necks are 1.45 and 1.03 times that of the normal subject.

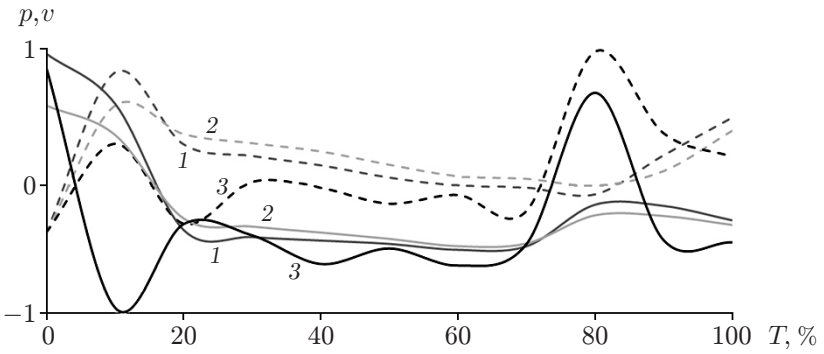

Fig. 4. Dimensionless velocity (dashed curves) and pressure (solid curves) during the cardiac cycle for the normal subject and two patients: patient with an aneurysm with a circular neck (*1*), patient with an aneurysm with an elliptical neck (*2*), and normal subject (*3*).

3. DISCUSSION AND CONCLUSIONS

As seen from the present results, the occurrence place of the maximum velocity, flow rate, and pressure of the blood flow for both patients and the normal subject are in the main artery. However, the occurrence place of the maximum WSS is in the aneurysm neck. The maximum blood velocity in the main artery of the patients is 23.1–34.7% higher than that of the normal subject. The blood pressure in the main artery of the patients with circular and elliptical necks is 36.7–46.5% higher than that of the normal subject. The maximum WSS values for the patients with circular and elliptical necks are higher than that for the normal subject by a factor of 6.5 and 4.1, respectively. Therefore, an increase in the WSS is an effective index for evaluation of blood hemodynamics in patients with a cerebral aneurysm.

3.1. Pulsatility of the Blood Flow

The Womersley number is the best index to evaluate the pulsatility of the fluid flow [16]. It is defined as

$$\mathrm{Wo} = R\sqrt{\omega/\nu}\,, \tag{2}$$

where R, ω, and ν are the aqueduct radius, the angular frequency, and the kinematic viscosity of blood, respectively.

At $\mathrm{Wo} < 1$, the flow profile is parabolic [17]. The maximum Womersley number is 3.3, 4.8, and 4.2 for the normal subject and patients with circular and elliptical necks, respectively. These results indicate the rise in the blood flow pulsatility by 28–45% after the occurrence of the disease.

It is known that there is a phase lag between the functions of the pressure gradient and velocity [17]. Figure 4 shows the dimensionless velocity and pressure during the cardiac cycle T for the normal subject and two patients. The phase lags between the blood pressure and blood velocity functions of the normal subject and patients B and C are 37.8°, 58.3°, and 46.4°, respectively. It should be noted that the Womersley number was determined in accordance with definition (2) under the assumption of non-deformable vessel walls. In the present study, however, the vessel walls are deformable.

3.2. Prediction of Aneurysm Rupture

The risk of aneurysm rupture is an essential concern for neurologists. As mentioned above, the WSS increases after the occurrence of the disease, resulting in vessel expansion. After the occurrence of an aneurysm, the volume of the aneurysm area for the patient with a circular neck is approximately 9% higher than that for the patient with an elliptical neck. The maximum displacements of the vessel wall in the peak systolic phase of the cardiac cycle for the normal subject and patients B and C are 0.2, 1.4, and 1.2 mm, respectively. Therefore, merely based on the geometric change in the aneurysm size, it can be claimed that the risk of vessel rupture for patients with a circular neck is higher than that for patients with an elliptical neck. However, the aneurysm rupture risk is also affected by other factors, such as the rate of thrombosis, gender of the patient, his/her individual features, family history,

smoking, alcohol consumption, etc. [18]. If the stress in the vessel walls is higher than the vessel strength, the rupture prediction index can be calculated as

$$I_{\mathrm{RP}} = \frac{\tau}{\tau_*} \cdot 100 \tag{3}$$

(τ is the stress in the vessel walls and τ_* is the vessel strength). The wall stress in Eq. (3) is calculated by using the ABAQUS software. The maximum wall stresses for the patients suffering from a cerebral aneurysm with circular and elliptical necks are 85.9 and 50.8 N/cm^2, respectively. The wall strength can be calculated by the formula [19]

$$\tau_* = 71.9 - 37.9(h_{\mathrm{th}}^{1/2} - 0.81) - 15.6(d - 2.46) - 21.3k + 19.3S,$$

where h_{th} is the thickness of the thrombus created in the aneurysm area, which was $h_{\mathrm{th}} = 0.24$ cm for both patients, d is the ratio of the vessel diameter without the aneurysm to the diameter of the aneurysm sphere, k is a coefficient representing the patient's family history ($k = 0.5$ if the patient has a family history in terms of the cerebral aneurysm disease and $k = -0.5$ if there is no family history), and S is a parameter whose value depends on the patient's gender ($S = 0.5$ if the patient is a man and $S = -0.5$ is the patient is a woman). It should be noted that both examined patients in the present study were men, each having the value $k = -0.5$. The rupture prediction index was $I_{\mathrm{RP}} = 77.4\%$ and $I_{\mathrm{RP}} = 45.8\%$ for the patients with circular and elliptical necks, respectively. As a result, other conditions being identical, the probability of aneurysm rupture for the patient with a circular neck is 40.8% higher than that for the patient with an elliptical neck.

REFERENCES

1. S. Omodaka, H. Endo, K. Niizuma, et al., "Quantitative Assessment of Circumferential Enhancement Along the Wall of Cerebral Aneurysms Using MR Imaging." Amer. J. Neuroradiol. **37** (7), 1262–1266 (2016).
2. M. Sanchez, O. Ecker, D. Ambard, et al., "Intracranial Aneurysmal Pulsatility as a New Individual Criterion for Rupture Risk Evaluation: Biomechanical and Numeric Approach (IRRAS project)," Amer. J. Neuroradiol. **35** (9), 1765–1771 (2014).
3. D. A. Steinman, J. S. Milner, C. J. Norley, et al., "Image-Based Computational Simulation of Flow Dynamics in a Giant Intracranial Aneurysm," Amer. J. Neuroradiol. **24** (4), 559–566 (2003).
4. M. Shojima, M. Oshima, K. Takagi, et al., "Magnitude and Role of Wall Shear Stress on Cerebral Aneurysm Computational Fluid Dynamic Study of 20 Middle Cerebral Artery Aneurysms," Stroke **35** (11), 2500–2505 (2004).
5. A. Valencia, A. Zarate, M. Galvez, et al., "Non-Newtonian Blood Flow Dynamics in a Right Internal Carotid Artery with a Saccular Aneurysm," Int. J. Numer. Methods Fluids **50** (6), 751–764 (2006).
6. K. Hajirayat, S. Gholampour, A. S. Seddighi, et al., "Evaluation of Blood Hemodynamics in Patients with Cerebral Aneurysm," Int. Clinic. Neurosci. J. **3** (1), 44–50 (2016).
7. A. Valencia, D. Ledermann, R. Rivera, et al., "Blood Flow Dynamics and Fluid-Structure Interaction in Patient-Specific Bifurcating Cerebral Aneurysms," Int. J. Numer. Methods Fluids **58**, 1081–1100 (2008).
8. H. Baek, M. V. Jayaraman, P. D. Richardson, et al., "Flow Instability and Wall Shear Stress Variation in Intracranial Aneurysms," J. Roy. Soc. Interface **7** (47), 967–988 (2009).
9. W. Brinjikji, H. J. Cloft, and D. F. Kallmes, "Difficult Aneurysms for Endovascular Treatment: Overwide or Undertall?" Amer. J. Neuroradiol. **30** (8), 1513–1517 (2009).
10. E. Yu. Meshcheryakova, "New Steady and Self-Similar Solutions of the Euler Equations," Prikl. Mekh. Tekh. Fiz. **44** (4), 3–9 (2003) [J. Appl. Mech. Tech. Phys. **44** (4), 455–460 (2003)].
11. S. V. Meleshko and V. V. Pukhnachev, "One Class of Partially Invariant Solutions of the Navier–Stokes Equations," Prikl. Mekh. Tekh. Fiz. **40** (2), 24–33 (1999) [J. Appl. Mech. Tech. Phys. **40** (2), 208–216 (1999)].
12. S. Gholampour, N. Fatouraee, A. S. Seddighi, and A. Seddighi, "Evaluating the Effect of Hydrocephalus Cause on the Manner of Changes in the Effective Parameters and Clinical Symptoms of the Disease," J. Clinic. Neurosci **35**, 50–55 (2017).
13. H. Li, K. Lin, and D. Shahmirzadi, "FSI Simulations of Pulse Wave Propagation in Human Abdominal Aortic Aneurysm: The Effects of Sac Geometry and Stiffness," Biomed. Eng. Comput. Biology **7**, 25–36 (2016).
14. S. S. Shishir, M. A. K. Miah, A. K. M. S. Islam, and A. B. M. T. Hasan, "Blood Flow Dynamics in Cerebral Aneurysm—A CFD Simulation," Proc. Eng. **105**, 919–927 (2015).

15. R. Torii, M. Oshima, T. Kobayashi, et al., "Fluid–Structure Interaction Modeling of a Patient-Specific Cerebral Aneurysm: Influence of Structural Modeling," Comput. Mech. **43** (1), 151–159 (2008).
16. S. Gholampour, N. Fatouraee, A. S. Seddighi, et al., "A Hydrodynamical Study to Propose a Numerical Index for Evaluating the CSF Conditions in Cerebralventricular System," Int. Clinic. Neurosci. J. **1** (1), 1–9 (2014).
17. S. Gholampour, N. Fatouraee, A. S. Seddighi, et al., "Numerical Simulation of Cerebrospinal Fluid Hydrodynamics in the Healing Process of Hydrocephalus Patients," Prikl. Mekh. Tekh. Fiz. **58** (3), 12–18 (2017) [J. Appl. Mech. Tech. Phys. **58** (3), 386–391 (2017)].
18. M. Xenos, S. H. Rambhia, Y. Alemu, et al., "Patient-Based Abdominal Aortic Aneurysm Rupture Risk Prediction with Fluid Structure Interaction Modeling," Ann. Biomed. Eng. **38** (11), 3323–3337 (2010).
19. J. P. V. Geest, D. H. J. Wang, S. R. Wisniewski, et al., "Towards a Noninvasive Method for Determination of Patient-Specific Wall Strength Distribution in Abdominal Aortic Aneurysms," Ann. Biomed. Eng. **34** (7), 1098–1106 (2006).